REPORT CRPL-9-8 ISSUED OCTOBER 4, 1948

U. S. DEPARTMENT OF COMMERCE
NATIONAL BUREAU OF STANDARDS
CENTRAL RADIO PROPAGATION LABORATORY
WASHINGTON, D. C.

A STANDARD OF ATTENUATION FOR MICROWAVE MEASUREMENTS

BY R. E. GRANTHAM AND J. J. FREEMAN

Reprinted from
TRANSACTIONS of the American
Institute of Electrical Engineers
Volume 67, page 535, 1948

A Standard of Attenuation for Microwave Measurements

R. E. GRANTHAM
NONMEMBER AIEE

J. J. FREEMAN
NONMEMBER AIEE

IN LINE with the program of the National Bureau of Standards for extending the standards of electrical quantities up through microwaves, the establishment of a standard of attenuation was undertaken. For such a standard to be useful, it must be readily adaptable to the calibration of commercial attenuators over the entire frequency range. Also, for self-consistency, such a standard must be capable of being checked by d-c measurements, thus relating the radio-frequency (r-f) standard to the more accurate primary standards.

A standard of any physical quantity consists not merely in the unique specification of that particular quantity, but equally important, in the specification of the operations, or procedures, through which an unknown quantity is measured in terms of it. The purpose of this paper is to describe such a standard, and the preliminary experiments employed in its evaluation and development.

General Description

Because of the extremely wide frequency range over which attenuators must be calibrated, the construction of a series of standard microwave attenuators to cover the entire spectrum, and the use of the direct substitution method of calibration, is impracticable. A modification of direct substitution, namely, the heterodyne or intermediate-frequency (i-f) substitution method, has been developed in various laboratories,[1,2] and permits the comparison of an unknown attenuator, operating at an arbitrary frequency, with a standard attenuator, operating at a fixed frequency. Thus, one standard attenuator, operating at a convenient frequency, may be used to calibrate attenuators over the entire microwave spectrum.

Essentially, the heterodyne method operates as follows. A r-f generator feeds power through an unknown attenuator into a linear frequency converter, which converts the microwave frequency into the intermediate frequency. The converter feeds through an i-f standard attenuator into an amplifier followed by a detector and meter. The unknown attenuator is then removed, and the standard attenuator adjusted to give the same meter reading. The attenuation of the unknown is then equal to the increase of attenuation of the standard.

This method assumes that the frequency converter is linear, that is, that the i-f power from the converter is proportional to the input microwave power. For small enough input power this is true for a crystal converter, and the operating conditions for a prescribed departure from linearity may be determined experimentally.

The range of attenuation which may be measured by the heterodyne method is less than that measurable by direct substitution, since in the heterodyne method the maximum permissible power input into the converter is limited by the advent of converter nonlinearity. However, a combination of direct substitution, using a previously calibrated r-f attenuator, together with the heterodyne method, extends the heterodyne attenuation range to that of the direct substitution method, although with a decrease in accuracy.

Detailed Description of the Equipment Used to Evaluate the Heterodyne Method at X-Band

The block diagram of the equipment used to evaluate the heterodyne method is shown in Figure 1. The r-f generator is a klystron providing at least 250 milliwatts of r-f power. The d-c power supplies for the klystron and amplifying circuits are battery-stabilized, rather than voltage-regulator-tube stabilized, and stabilized, and special shock mountings are used to prevent noise modulation of the r-f signal by the blower used to cool the klystron. A very high degree of amplitude stability is necessary in all of the components of the system, because the output meter of the system is sensitive to a 0.2 per cent (0.01 decibel) change in power level.

The frequency of the r-f generator is measured by a calibrated wavemeter in the spectrum analyzer. The amplitude of the r-f output of the generator is monitored by a unit as shown in Figure 2. A sensitive d-c galvanometer in the power monitor gives a unit scale deflection for a 0.05 per cent (0.002 db) change in power level. Variable attenuator A, in Figure 1, is used to calibrate the power monitor.

The r-f generator klystron is followed by buffer attenuator B which prevents changes in impedance caused by inserting and removing the unknown attenuator from changing the load impedance presented to the klystron. Thus the power output and frequency of the r-f generator are maintained constant throughout a measurement. A twenty-db attenuator provides an adequate amount of buffing, as evidenced by the fact that the introduction of a 10 to 1 voltage standing-wave ratio at transformer A resulted in no change of generator output, as indicated by the power monitor.

When measuring the insertion loss of

Paper 48-50, recommended by the AIEE instruments and measurements committee and approved by the technical program committee for presentation at the AIEE winter general meeting, Pittsburgh, Pa., January 26–30, 1948. Manuscript submitted November 12, 1947; made available for printing December 15, 1947.

R. E. GRANTHAM and J. J. FREEMAN are both with the National Bureau of Standards, Washington, D. C.

The authors wish to express appreciation for the valuable services of R. H. McCracken who constructed much of the electronic equipment and performed many of the experiments, and A. A. Feldmann who designed the mechanical features of the wave-guide-below-cutoff attenuator.

Figure 1. Block diagram of the intermediate-frequency method of attenuation measurement

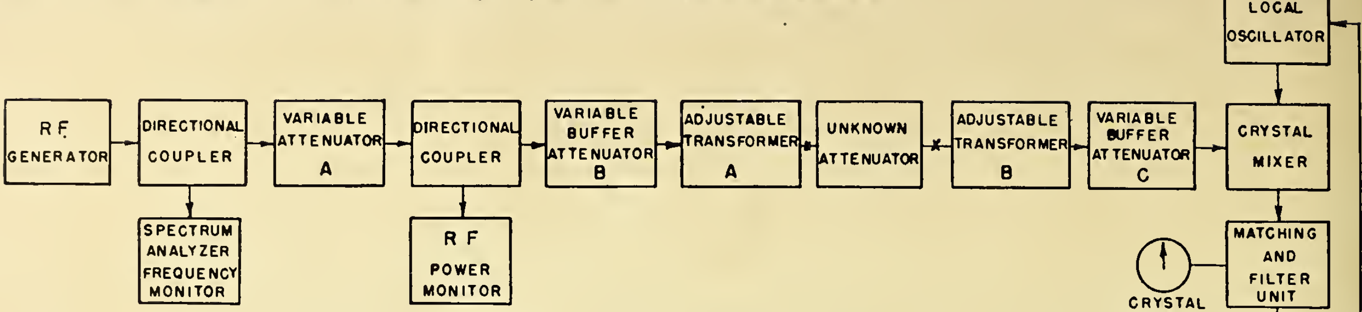
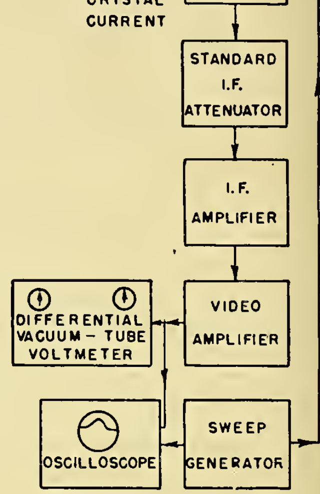

Figure 2. Radio-frequency power monitor schematic

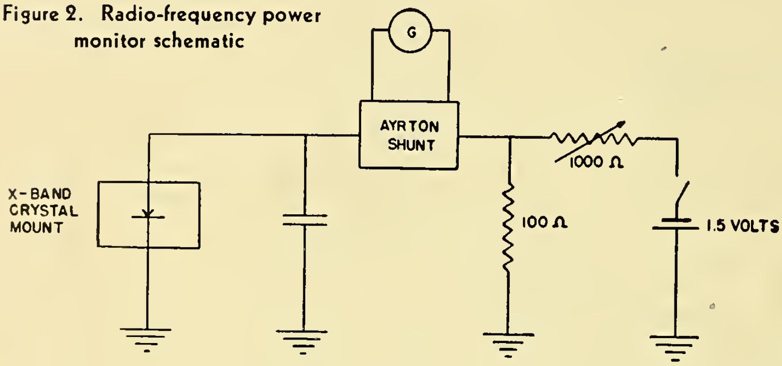

an attenuator, it is necessary to insert the attenuator in a transmission line which is matched looking both ways from the point of insertion. To meet this requirement it is necessary to use adjustable transformers *A* and *B* to match attenuators *B* and *C* respectively as accurately as possible to the characteristic impedance of the wave guide.

Buffer attenuator *C* is needed to isolate the local oscillator from the changes in the impedance of its load which would occur when the unknown attenuator is inserted and removed. The conversion efficiency of the crystal changes appreciably with local-oscillator power. Hence, the local-oscillator power output must be maintained as constant as possible. Twenty db is the minimum attenuation used for buffer attenuator *C*.

The repeller voltage of the local-oscillator klystron is swept by a linear sawtooth voltage so that the beat-frequency output of the mixer sweeps over about 0.5 megacycles per second. The i-f amplifier band width is about 50 kilocycles per second, so the i-f response curve is plotted on the oscilloscope as in the usual spectrum analyzer, but with much more than the usual frequency dispersion. The peak voltage of the pulse on the oscilloscope is measured by a differential vacuum-tube voltmeter, which has a sensitivity of one scale division per 0.2 per cent (0.01 db) change in power level. The reason for sweeping the local-oscillator frequency rather than operating it continuous wave (c-w) is that small shifts in the frequency of the r-f generator or the local oscillator may occur up to about 200 kilocycles per second without causing appreciable variations in the output differential voltmeter. If the local oscillator were operated c-w, the beat frequency could not vary more than about plus or minus 3 kilocycles per second for the same variations in output.

Range of Measurement and Errors of Heterodyne Method

The attenuation range measurable by the heterodyne method is determined by the maximum input power consistent with crystal linearity, and by the crystal noise power. The range of crystal linearity was determined by measuring a fixed value of attenuation as a function of crystal input power, using the apparatus indicated in Figure 3. The measured values of attenuation of a 30-db pad as a function of r-f buffing, and hence crystal input power, are depicted in Figure 4. For 100 milliwatts of r-f input power, it appears that 40 db of buffing attenuation (corresponding to a crystal input power of 10 microwatts) suffices for accuracies of plus or minus 0.02 db.

The crystal noise power was measured to be less than one micromicrowatt. Accordingly, the maximum range of attenuation measurement corresponding to an error of 0.05 db due to crystal noise, is 50 db.

In addition to possible crystal nonlinearity, errors in the heterodyne method may occur through r-f or i-f leakage, mismatch on either side of the r-f or i-f attenuators, frequency and amplitude instability and errors in the i-f standard attenuator. Errors of the i-f standard will be discussed in another paragraph, and the question of errors due to mismatch is too lengthy and detailed to consider at this time. If we neglect the last two sources of error, the over-all accuracy of attenuation measurements with the equipment described herein is estimated to be within plus or minus 0.02 db in the 0-10 db range, and plus or minus 0.2 per cent of the attenuation value in db for the 10-50 db range.

Theoretical Factors Affecting the Choice and Design of the Attenuator

To be suitable as a standard, the i-f attenuator must be able to yield known values of attenuation in terms of an accurately measurable parameter, such as length, or it must be capable of calibration in terms of d-c measurements. First designed by Harnett and Case,[3] the cutoff attenuator, Figure 6, which consists of a hollow tube excited at one end below its cutoff frequency, and a coil or condenser which picks up the attenuated field at the other end, fulfills the former requirement. Since the generated field falls off exponentially with distance from the exciting source, and since the attenuation constant may be computed from the dimensions of the tube, the ratio of any two voltages, or the attenuation introduced by a given length of tube, is reduced to a measurement of length.

Cross-Section of Tube

However, it is well known that the electromagnetic field generated within the tube consists of the superposition of an infinite number of modes, each of which is attenuated along the axis of the tube as $e^{-\alpha_{nm}z}$, where α_{nm} is a function of the geometry of cross section, and the particular mode. The higher the mode, the greater is its attenuation constant α_{nm}, so that only for large enough values of z do the higher modes become negligible. Obviously, then, the accuracy of the attenuator increases as the ratios of the amplitudes of the higher modes to that of the lowest one decrease, and as the ratios of the attenuation constants of the higher modes to that of the lowest one increase. The comparison of these factors for tubes of circular and rectangular cross section is given in Table I.

Circular Cross Section. The fifth column of Table I enumerates the ratio of attenuation constants, α_{nm}, of the first few modes to that of the lowest mode, for circular cross-section.

From Table I, it is apparent that a measure of purity of mode can be achieved by exciting the TE_{11} mode, and by eliminating the TE_{01}, TE_{21}, and TM_{01} modes through symmetry of excitation. Just as a violin string plucked in the center does not vibrate with even harmonic modes similarly, a proper symmetry of the exciting current distribution in a cutoff attenuator will not excite certain classes of modes. In particular, if one considers the cross section divided into four symmetrical quadrants, and if the current distribution in the right-hand quadrants is the negative mirror image of that in the left-hand quadrants, and if the current distribution in the upper quadrants is the positive mirror image of that in the lower quadrants, then only those modes will be excited for which n, (the mode index indicating angular dependence) is odd, eliminating five of the seven undesired modes listed in the column. However, if one uses an unbalanced generator to excite the attenuator coil, the distributed capacitance of the coil makes the achievement of this symmetry difficult.

The obvious type of exciting symmetry associated with a circular tube is, of course, circular symmetry. In particular, circularly-symmetric capacitative disk excitation, described by Harnett and Case[3] and W. O. Smith[4] will excite only transverse magnetic modes, for which $n=0$; of these the mode with the lowest attenuation constant is the TM_{01}. The danger with this type of attenuator is that any asymmetry will produce a TE_{11} mode which has a lower attenuation constant, and hence, for a large enough value of attenuation, can lead to appreciable error.

Rectangular Cross Section. The first four columns of Table I enumerate the ratios of attenuation constants, α_{nm}, of the first few modes to that of the lowest mode, for several ratios of rectangular cross-section dimensions, a and b. It will be noticed that for $a=b/2$, or less, the unwanted modes decay much faster than for circular cross-section. Also, if the exciting-current distribution is chosen so that to each element of current corresponds its negative mirror image with respect to the plane $x=a/2$, and its positive mirror image with respect to the plane $y=b/2$, then it may be shown that only those modes are excited for which m is even and n is odd. Although this type of symmetry is difficult to achieve at lower frequencies, using coil structures, at microwave frequencies this type of symmetry should be easily obtainable using symmetric windows as the exciting structures.

Reaction Effect

The reaction of the receiver circuit on the exciting current becomes the limiting factor affecting the closeness of spacing between exciter and receiver, when precautions have been taken to reduce the unwanted modes, since exponential decay with spacing implies constant current or voltage excitation, for the TE_{11} and TM_{01} modes respectively. As already mentioned by Harnett and Case,[3] the impedance coupled into the exciter circuit by the receiver decreases as $e^{-2\alpha_{11}z}$ for the TE_{11} mode, and as $e^{-\alpha_{01}z}$ for the TM_0 mode, where z is the separation between exciter and receiver. Accordingly, a further advantage of the TE_{11} mode over the TM_{01} mode attenuator is the smaller interaction between exciting and receiving circuits for a given attenuation.

Skin Effect

For a perfectly conducting circular tube, of radius a,

$$\alpha_{11}=\frac{1.841}{a}\left[1-\left(\frac{2\pi}{1.841}\frac{a}{\lambda}\right)^2\right]^{1/2} \quad \text{for the } TE_{11} \text{ mode} \quad (1)$$

$$\alpha_{01}=\frac{2.405}{a}\left[1-\left(\frac{2\pi}{2.405}\frac{a}{\lambda}\right)^2\right]^{1/2} \quad \text{for the } TM_{01} \text{ mode} \quad (2)$$

If one takes into account the effect of finite conductivity, σ, following the method of Stratton,[6] one gets easily, for the attenuation constans.

$$\alpha'_{11}=\frac{1.841}{a}\left[1-\frac{\delta}{a}+\left(\frac{2\pi}{1.841}\frac{a}{\lambda}\right)^2\right]^{1/2} \quad \text{for the } TE_{11} \text{ mode} \quad (3)$$

$$\alpha'_{01}=\frac{2.405}{a}\left[1-\left(\frac{2\pi}{2.405}\frac{a}{\lambda}\right)^2\left(1+\frac{\delta}{a}\right)\right]^{1/2} \quad \text{for the } TM_{01} \text{ mode} \quad (4)$$

where $\delta=\left(\frac{2}{\omega\mu\sigma}\right)^{1/2}$ is thd skin depth.

For an i-f attenuator, $a/\lambda << 1$, and it is seen that there is no correction for the TM_{01} mode, whereas the effects of finite conductivity are such as to increase the effective radius from a to $a+(\delta/2)$, for the TE_{11} mode.

Figure 3. Buffing block diagram for measuring crystal nonlinearity

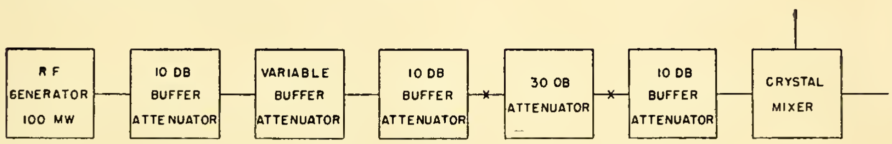

Table I

Mode	Rectangular Wave Guide $\alpha/\alpha TE_{01}$	$\alpha/\alpha TE_{01}$	$\alpha/\alpha TE_{01}$	$\alpha/\alpha TE_{01}$	Circular Wave Guide $\alpha/\alpha TE_{11}$	Mode
	a = b	a = 0.9b	a = b/2	a = b/3		
TE_{01}	1.0	1.0	1.0	1.0	1.0	TE_{11}
TE_{02}	2.0	2.0	2.0	2.0	1.31	TM_{01}
TE_{03}	3.0	3.0	3.0	3.0	1.66	TE_{21}
TE_{10}	1.0	1.1	2.0	3.0	2.08	TE_{01}, TM_{11}
TE_{20}	2.0	2.2	4.0	6.0	2.79	TM_{21}
TE_{11}, TM_{11}	1.41	1.5	2.2	3.1	2.90	TE_{12}
TE_{21}, TM_{21}	2.2	2.4	4.1	6.1	3.0	TM_{02}

Experimental Evaluation of Cutoff Attenuator

Mechanical Description

A circular waveguide-below-cutoff attenuator was built for operation at 20 megacycles per second, with the TE_{11} mode having an attenuation rate of 21 db per inch. The distance between coils is adjusted by a mechanical screw drive, and a mechanical counter reads the attenuation directly in units of 0.01 db. Rectangular coils mounted on precision-made bakelite forms are used in an effort to secure symmetry in the generation of the TE_{11} mode, and hence reduce the unwanted modes. The mechanical precision of construction is such that the accuracy of attenuation reading is ±0.01 db per inch.

Early experiments with the attenuator revealed that it could not be set to a given attenuation value within plus or minus 0.1 db. The fingers on the moving plunger, as shown in Figure 6, were replaced by helical spring fingers, as described by Sydoriak[2] but with no improvement. Finally, the contacts were removed entirely, and the plunger which supported the coil was constructed of bakelite, eliminating the variable attenuation value for a given setting.

Linearity of Attenuator

Direct Measurement of Attenuator Linearity. In order to check the linearity of the attenuator, that is, the deviation of its rate of attenuation from $e^{-\alpha_{11}z}$, the measurement setup illustrated in Figure 5 was used. The exciting coil in Figure 6 was connected to the i-f signal generator, and the receiving coil was matched to 50 ohms by inserting a resistor and capacitor in series with the coil, and tuning for resonance.

Measurements of the attenuation of a particular 5-db step of the Leeds and Northrup carbon attenuator were made for different separations of the coils in the cutoff attenuator, and were found to be constant within experimental error (plus or minus 0.01 db), for coil separations greater than 20 db (about 1 inch). For smaller separations, the measured values of attenuation were variable, depending upon the angle between the axes of the coils. This departure from linearity was caused partly by the change in exciting current due to coupled impedance of the secondary coil, and partly by the presence of higher order modes.

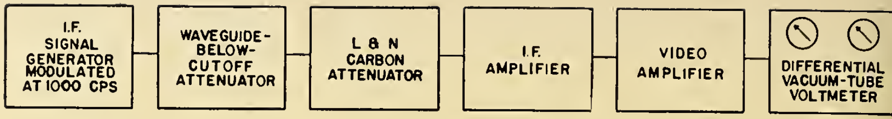

Figure 5. Intermediate-frequency measurement setup for comparing wave-guide-below-cutoff attenuator with Leeds and Northrup carbon attenuator

Measurement of Relative Amplitudes of Higher Modes. The first few higher modes, the TM_{01}, TE_{21}, TM_{11}, and TE_{01}, have attenuation rates of 28, 35, 44, and 44 db per inch, respectively, in the experimental cutoff attenuator. For large enough coil separations the preponderant higher mode will be the TM_{01}, since its attenuation rate is not so very different from that of the TE_{11}. For this condition, a method of measuring the relative amplitudes of the TE_{11} and TM_{01} modes by utilizing their different angular dependence was described by Sydoriak,[2] and developed by Griesheimer.[5] This method assumes that

1. Only the TM_{01} and TE_{11} modes are present in sufficient strength to be of importance.
2. Transfer impedance effects are negligible.
3. The tube cross section has no elliptical eccentricity.

It follows from waveguide theory that the voltage induced in the receiving coil from the TE_{11} mode varies as the cosine of the angle, θ, between the axes of the coils, and that induced from the TE_{01} mode is independent of angle. Then, let

$$V_{TE}=A_1e^{-\alpha_{11}z}\cos\theta \qquad (5)$$

$$V_{TM}=A_2e^{-\alpha_{01}z} \qquad (6)$$

represent the voltage induced in the receiving coil by the TE_{11} and TM_{01} modes, respectively, where z represents the distance between the coils.

Since these voltages are separated in time phase by an angle ζ which is approximately 180 degrees, the resultant voltage amplitude is given by

$$V^2=V_{TE}^2+V_{TM}^2+2V_{TE}V_{TM}\cos\zeta \qquad (7)$$

This may also be written

$$V^2=(A_1e^{-\alpha_{11}z})^2[1+r^2e^{-2bz}+2re^{-bz}\cos\theta\cos\zeta-\sin^2\theta] \qquad (8)$$

where

$$r=\frac{A_2}{A_1} \qquad (9)$$

and

$$b=\alpha_{01}-\alpha_{11} \qquad (10)$$

If we keep z constant, and vary θ, V^2 will have a maximum, $V^2_{\max}$, at $\theta=\pm\pi$, and a secondary maximum, V^2_{submax} at $\theta=0$, and a minimum, $V^2_{\min}$, at $\cos\theta'=-re^{-bz}\cos\zeta$. If we assume the coils are adjusted for maximum power transfer, $\theta=\pi$, then it follows from equation 8 that the attenuation in decibels introduced by displacing the secondary coil from an initial separation, z_o, between coils to a final separation z, is given by

$$A_{db}=10\log_{10}\exp(-2\alpha_{11}[z_0-z])+10\log_{10}\frac{1+r^2\exp(-2bz_0)-2r\exp(-bz_0)\cos\zeta}{1+r^2\exp(-2bz)-2r\exp(-bz)\cos\zeta} \qquad (11)$$

From equation 11, it is seen that the presence of the TM_{01} mode introduces a deviation from the exponential law of decay which obtains when only the TE_{11} mode is present. If we define this deviation of the actual attenuation in decibels from the theoretical exponential value as the error, E_{db}, due to the TM_{01} mode, it follows from equation 11 that the maximum error in a measurement of attenuation where the minimum separation between coils is z_o, is

$$E_{db}=10\log_{10}[1+r^2\exp(-2bz_0)-2r\exp(-bz_0)\cos\zeta] \qquad (12)$$

The value of E_{db} for a given minimum

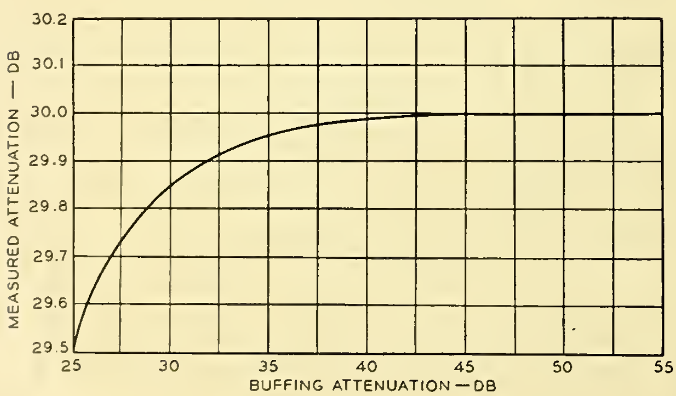

Figure 4. Measured attenuation of nominal 30-db radio-frequency attenuator as a function of total buffing attenuation using 100 milliwatts of input power

A buffing attenuation of 40-db corresponds to a crystal input power of 10 microwatts

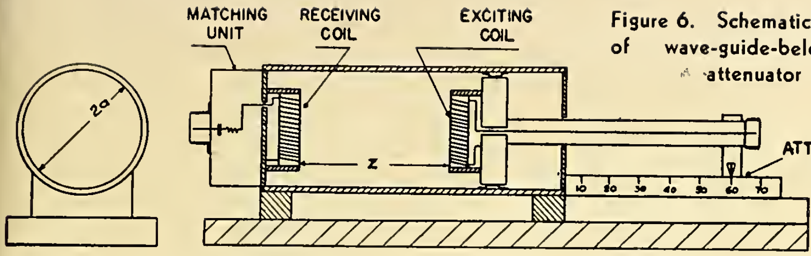

Figure 6. Schematic diagram of wave-guide-below-cutoff attenuator

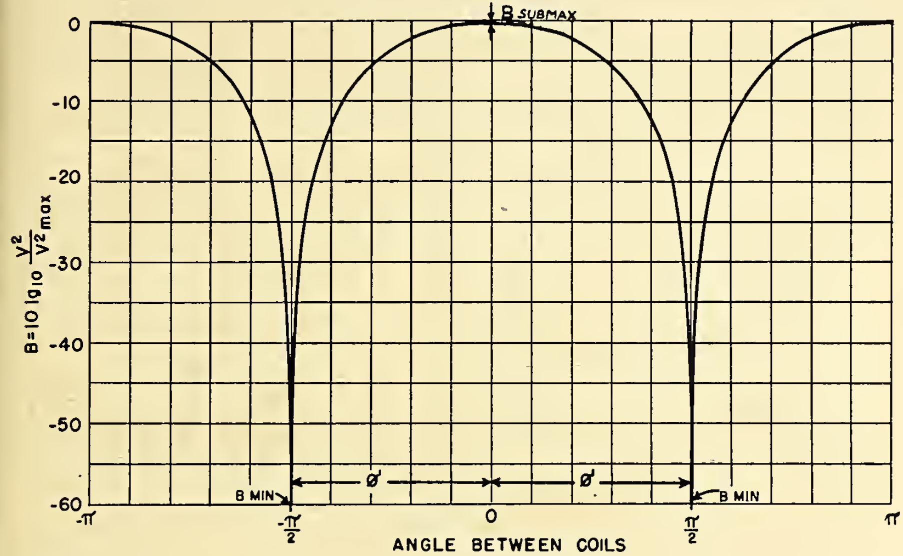

Figure 7. Graph of B = 10 log (V^2/V^2_{max} as a function of angular rotation of coils for TE_{11} mode circular attenuator

separation between coils may be determined experimentally by measuring

$$\frac{V^2_{submax}}{V^2_{max}}$$

and

$$\frac{V^2_{min}}{V^2_{max}}$$

at the coil separation z_o.

It is convenient to define the following quantities:

$$B = 10 \log_{10} \frac{V^2}{V^2_{max}} \tag{13}$$

$$B_{submax} = 10 \log \frac{V^2_{submax}}{V^2_{max}} \tag{14}$$

$$B_{min} = 10 \log_{10} \frac{V^2_{min}}{V^2_{max}} \tag{15}$$

$$\frac{V^2_{submax}}{V^2_{max}} = h^2$$

$$\frac{V^2_{min}}{V^2_{max}} = \beta^2 \tag{16}$$

Figure 7 is a typical plot of B as a function of angle between the axes of the coils, and illustrates the power coupled into the receiving coil as a function of angle of rotation, between the coils. If the two values of B_{min} in Figure 7 are not the same, then a third mode must be present. Also if the minimum points are not displaced by equal angles to either side of B_{submax}, a third mode must be present. Using the measured values of B_{submax} and B_{min} as defined herein, the values for r and ζ may be determined from the following equations, as derived by Griesheimer.[5]

$$J = \left[\frac{h^2 - \beta^2}{1 - \beta^2}\right]^{1/2} \tag{17}$$

$$re^{-bz_0} = \frac{1-J}{1+J}\left[1 + \frac{4\beta^2}{1-h^2}\,\frac{(1+J)}{(1-J)}\right]^{1/2} \tag{18}$$

$$\cos \zeta = -\left[1 + \frac{4\beta^2}{1-h^2}\,\frac{(1+J)}{(1-J)}\right]^{-1/2} \tag{19}$$

$$\cos \theta' = \frac{(1-J)}{(1+J)} \tag{20}$$

Measurements on the experimental TE_{11} mode cutoff attenuator, using rectangular coils, showed that the angular calibration was symmetrical within the accuracy of the measurement, and it was concluded that there was no appreciable coupling due to modes higher than the TM_{01}. The value of B_{submax} was found to be -0.30, and the value of B_{min} to be -60. From equations 16–20 the following values of r, ζ, and θ' were obtained $re^{-bz_0} = 0.017$, $\zeta = 176.5$ degrees, and $\theta' = 89$ degrees.

The maximum error in attenuation, E_{db}, for this separation was therefore, from equation 12, 0.14 db. For a minimum coil separation corresponding to an attenuation of 20 db, the maximum error

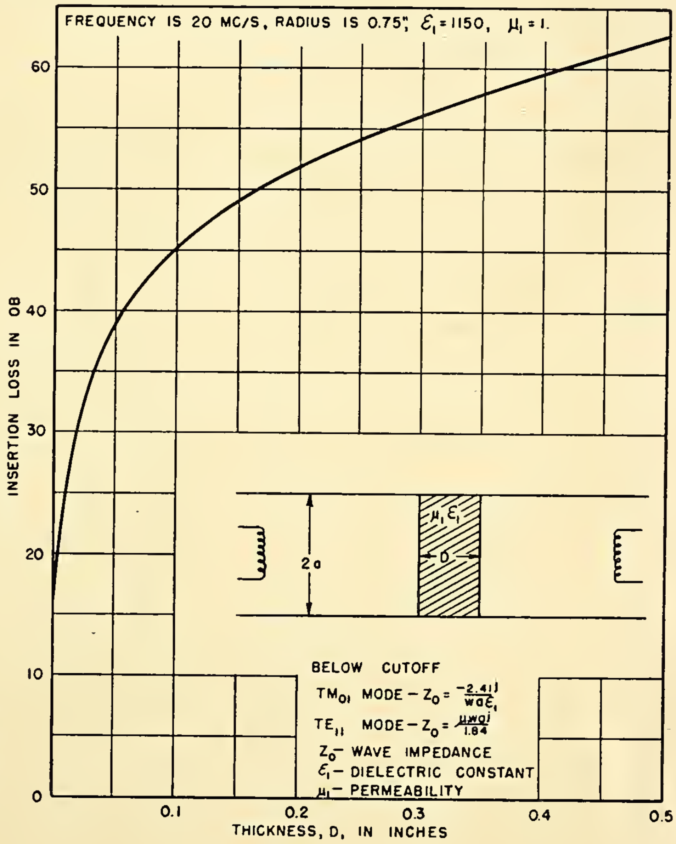

Figure 8. Calculated insertion loss of barium titanate disk for TM_{01} mode versus thickness of disk

in attenuation was 0.08 db. The latter error was not detected by measuring the 5-db step of the Leeds and Northrup attenuator because the error was spread over such a wide range of attenuation that the amount included in a 5-db interval was smaller than the experimental error.

Dielectric Filters. The equation for the *TM*-mode wave impedance, Z_{nm}, of a circular hollow tube of radius a, containing a medium of permeability, μ_1, and dielectric constant of ξ_1, is given by

$$Z_{nm}=\left[\left(1-\frac{f_{nm}^2}{f^2}\right)\left(\frac{\mu_1}{\xi_1}\right)\right]^{1/2} \tag{21}$$

This simplifies, at frequencies far below cutoff, to

$$Z_{nm}-\frac{-U_{nm}j}{2\pi fa\xi_1} \tag{22}$$

For *TE* waves, the wave impedance simplifies to:

$$Z_{nm}=\frac{a\mu_1 2\pi fj}{v_{nm}} \tag{23}$$

Here, f_{nm} and f are the cutoff and impressed frequencies, $j=\sqrt{-1}$, and U_{nm} and v_{nm} are numerical factors which depend upon the mode. Hence, a material of high dielectric constant will reflect the *TM* wave and pass unchanged the *TE* wave. The high dielectric constant material has a wave impedance, for the *TM* mode, inversely proportional to the dielectric constant so that a large discontinuity between air and the material would exist and cause reflections of the *TM* mode. The *TE* mode, on the other hand, would not be reflected because its wave impedance is independent of ξ_1. Similarly, a material of high permeability could be inserted in the guide to reflect the *TE* wave, but not reflect *TM* wave. The theoretical insertion loss for the TM_{01} mode of a barium titanate disk with a dielectric constant of 1,150 is plotted in Figure 8, as a function of its thickness.

The measured insertion loss of a barium titanate disk of 0.25 inches in thickness, having a dielectric constant of 1,150, was 40 db for the TM_{01} mode, and 0.05 db for the TE_{11} mode. To insure an intimate contact between the barium titanate and the inside surface of the cutoff attenuator, the rim of the disk was silvered.

The insertion loss of the barium titanate disk for the TM_{01} mode, and of other types of TM_{01} mode filters described in the following paragraph was measured by replacing the exciting coil in the circular attenuator by a capacitative exciting disk, which excited the TM_{01} mode primarily. At a fairly close spacing between the receiving coil and exciting disk, the

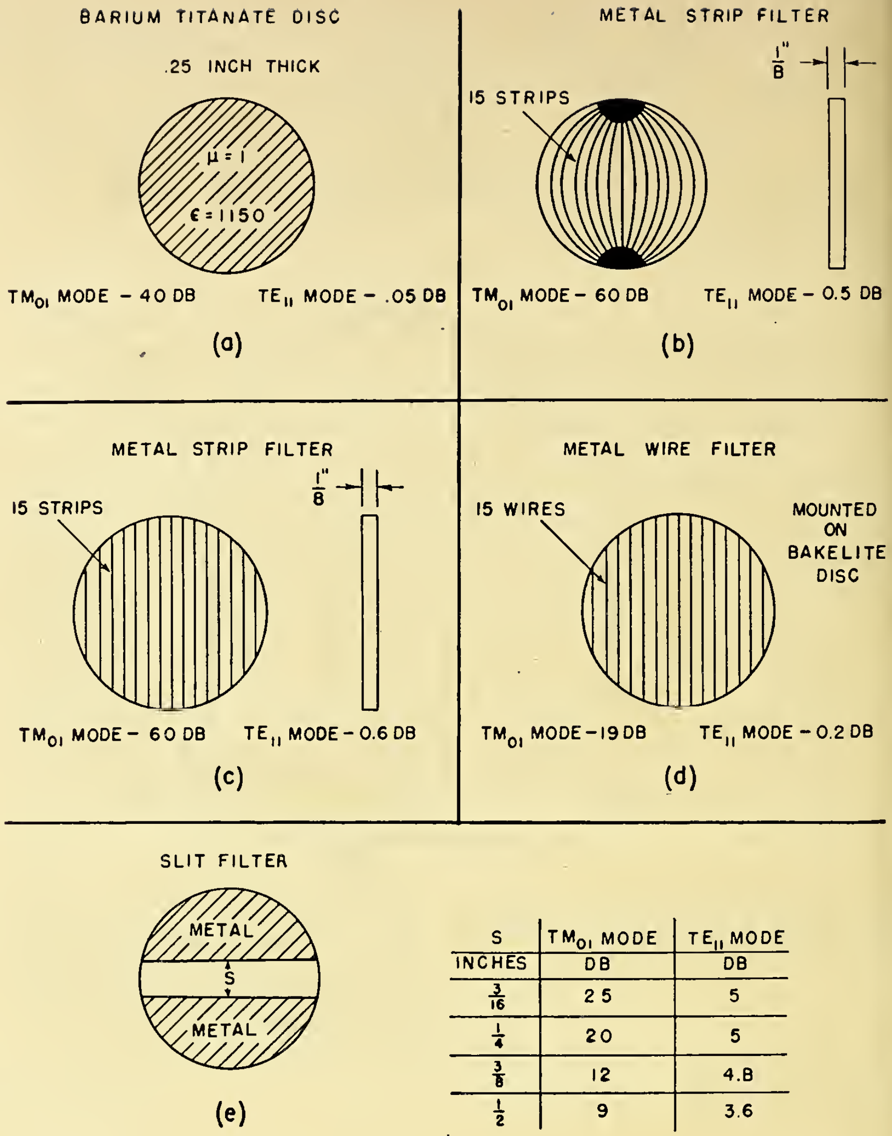

S INCHES	TM_{01} MODE DB	TE_{11} MODE DB
3/16	25	5
1/4	20	5
3/8	12	4.8
1/2	9	3.6

Figure 9. Insertion loss of various mode filters for TE_{11} and TM_{01} modes in cutoff attenuator

amplitude of the TE_{01} mode was measured to be less than 1/1,000 that of the TM_{01} mode. Thus there was ample range for measurement of TM_{01} insertion loss for various filters.

Metal Mode Filters. Various other types of filters illustrated in Figure 9 were tried. The slit filter, Figure 9e, was used by Sydoriak[2] at higher frequencies, but it is not the best type for i-f frequencies, as the data on Figure 9 indicate, because the slit filter reflects a considerable amount of the TE_{11} mode as well as the TM_{01} mode.

Gainsborough[1] developed the wire filter as shown in Figure 9d. It is not as effective as the copper-strip filter shown in Figure 9c. A little less insertion loss for the TE_{11} mode is obtained if the copper strips are bent so as to be approximately perpendicular to the electric lines of the TE_{11} mode as is shown in Figure 9b. Of course the filters in Figure 9b, c, d, and e must be properly oriented or they will reflect the TE_{11} mode as well as the TM_{01} mode.

Using the metal strip filter of Figure 9b an angular calibration of the cutoff attenuator was made. The value of B_{submax} was zero within limits of measurement, and B_{min} was less than -80.

Comparison With Leeds and Northrup Carbon Attenuator. A calibration of the Leeds and Northrup carbon attenuator was made over a 40-db range in attenuation at 20 megacycles per record. The resulting attenuation calibration checked within 0.03 db the calibration made with direct current. A check was then made by operating the cutoff attenuator as a TM_{01} attenuator as described previously for TM_{01} mode-filter insertion loss. The TM_{01} mode calibration was made at only two values of attenuation, 10 db and 20 db, and the values obtained checked the previous calibration within plus or minus 0.01 db.

Conclusion

The heterodyne or i-f substitution method of calibrating microwave attenuators has been investigated, and preliminary equipment has been built to utilize the method. The accuracy obtained is estimated to be within plus or minus 0.02 db in the 0–10 db attenuation range, and plus or minus 0.2 per cent of the attenuation value in db for the 10–50 db range, assuming unity standing-wave ratio presented to both sides of the attenuator under calibration. The basic standard of the heterodyne method is a waveguide-below-cutoff attenuator operated at an intermediate frequency. A preliminary model of an i-f standard cutoff attenuator has been built, tested, and improved until its accuracy is plus or minus 0.01 db per 20 db unit of attenuation.

References

1. A Method of Calibrating Standard-Signal Generators and Radio-Frequency Attenuators, **G. F. Gainsborough.** *Journal,* Institution of Electrical Engineers (London, England), volume 94, part 3, number 29, May 1947.

2. Radio-Frequency Attenuators, **S. G. Sydoriak.** *Radiation Laboratory Report 404* (Massachusetts Institute of Technology (Cambridge, Mass.), September 7, 1943.

3. The Design and Testing of Multirange Receivers, **D. E. Harnett, N. P. Case.** *Proceedings,* Institute of Radio Engineers (New York, N. Y.), volume 23, number 6, June 1935.

4. Capacitance Type Radio-Frequency Attenuators, **W. O. Smith.** *Radiation Laboratory Report* 995, Massachusetts Institute of Technology (Cambridge, Mass.), January 18, 1946.

5. Notes on TE_{11} Mode Cutoff Attenuators, **R. N. Griesheimer.** *Radiation Laboratory Report 55,* Massachusetts Institute of Technology (Cambridge, Mass.), November 16, 1944.

6. Electromagnetic Theory (book), **J. A. Stratton.** McGraw-Hill Book Company, New York, N. Y., 1941, page 543.

No Discussion

Preprinted from
TRANSACTIONS of the American
Institute of Electrical Engineers
33 West 39th St., New York, N. Y.

Printed in the United States of America

6/31/'48 Volume 67, 1948